ARTICLES

Photodissociation Dynamics of 1,3-Butadiene at 157 nm

Xiaolan Mu,[†] I-Chung Lu,[‡] Shih-Huang Lee,[§] Xiuyan Wang,[†] and Xueming Yang*[,†]

State Key Laboratory of Molecular Reaction Dynamics, Dalian Institute of Chemical Physics, Chinese Academy of Sciences, Dalian 116023, People's Republic of China, and Department of Chemistry, National Tsing Hua University, Hsinchu, Taipei, and Synchrotron Radiation Research Center, Hsinchu, Taiwan

Received: June 25, 2004; In Final Form: October 19, 2004

Photodissociation of 1,3-butadiene at 157 nm has been investigated using the photofragment translational spectroscopy technique. Tunable VUV synchrotron radiation was used for product photoionization detection. Six dissociation channels have been identified including $C_4H_5 + H$, $C_4H_4 + H_2$, $C_3H_3 + CH_3$, $C_2H_3 + C_2H_3$, $C_2H_4 + C_2H_2$, and $C_4H_4 + H + H$. The product kinetic energy distributions for all observed dissociation channels have been determined. The relative branching ratios for different channels are also estimated. It appears that the majority of the excited 1,3-butadiene molecules go through isomerization before they dissociate, while direct bond dissociation channels are less important in comparison with 1,2-butadiene photodissociation at the same excitation wavelength.

I. Introduction

Spectroscopy and photochemistry of unsaturated hydrocarbons have been extensively studied both experimentally and theoretically.[1−10] UV absorption spectra measured by McDiarmid show that 1,3-butadiene shows several Rydberg series between 2300 and 1350 Å.[1] Electronic transitions to the 3s Rydberg state (1^1B_g) at 6.22 eV, the two 3p Rydberg states at 6.66 and 7.07 eV, and the 4p Rydberg state at 8.00 eV have been identified. The ground state of 1,3-butadiene has the A_g symmetry, and the electronically excited states may have A_g, A_u, B_g, or B_u symmetry. For a single-photon process, transitions to an excited g symmetry state are not allowed from the ground A_g state, and only transitions to an A_u or B_u state are allowed. The B_u states are expected to be relatively intense since the transition dipole length can approach half the length of the π-system. The A_u transitions are expected to be relatively weak since the transition moment length in the *z* direction is small.[11] Therefore, the 157 nm excitation of 1,3-butadiene should be mainly via the electronic transition to the 3p Rydberg state, $1^1A_g \rightarrow 2^1B_u$.

Numerous studies on the photochemistry of 1,3-butadiene have been previously carried out. Photolysis of 1,3-butadiene by mercury photosensitization[12] or VUV light[13−17] shows clear evidence for three dissociation channels: $CH_3 + C_3H_3$, $C_4H_4 + H_2$, and $C_2H_4 + C_2H_2$. A series of shock tube pyrolysis studies[18−23] indicate that the first step in pyrolysis was dissociation to two vinyl radicals. Hidaka and co-workers[23] concluded that the $CH_3 + C_3H_3$ channel is the most important channel. All of these studies were carried out at relatively high pressures with multiple collisions during the course of the measurement. Valentini[24] have determined the (v, J) distribution of the H_2 photoproduct from butadiene photolysis at 212.8 nm under a collisionless condition. In a recent study by Robinson and co-workers,[25] photodissociation of 1,3-butadiene has been investigated at 193 nm. Five product channels have been observed: $CH_3 + C_3H_3$, $C_4H_5 + H$, $C_2H_3 + C_2H_3$, $C_4H_4 + H_2$, and $C_2H_4 + C_2H_2$.[25]

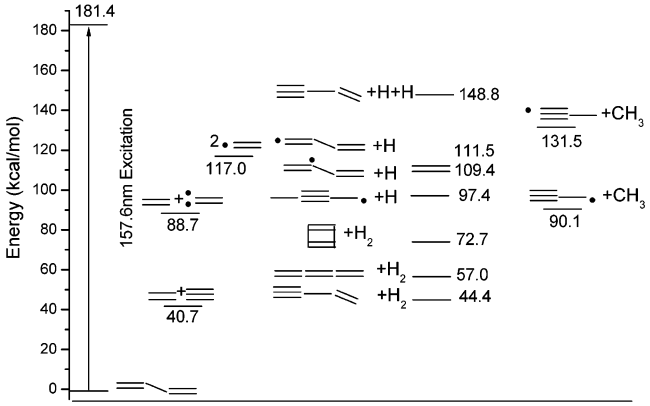

Figure 1. Energetics of photodissociation channels of 1,3-butadiene at 157 nm excitation.

In the present work, we have investigated the photodissociation of 1,3-butadiene at 157 nm in a collision-free environment using a molecular beam apparatus at the synchrotron radiation center in Hsinchu. The energetic diagram for possible dissociation channels from the photodissociation of 1,3-butadiene at 157 nm excitation is shown in Figure 1, which was constructed using previous theoretical and experimental results.[26−32] In this work, time-of-flight (TOF) spectra of photodissociation products are measured by the photofragment translational spectroscopic technique. Product kinetic energy

* To whom correspondence should be addressed. E-mail: xmyang@dicp.ac.cn.
[†] Chinese Academy of Sciences.
[‡] National Tsing Hua University.
[§] Synchrotron Radiation Research Center.

10.1021/jp047239c CCC: $27.50
Published on Web 12/04/2004

distributions are determined from the time-of-flight spectra of the photofragment. Relative contributions of different channels have also been estimated.

II. Experimental Section

Photodissociation of 1,3-butadiene has been carried out on a molecular beam apparatus capable of performing both crossed-beam molecular reaction and photofragmentation studies at the chemical dynamics beamline at the National Synchrotron Radiation Research Center (NSRRC) in Hsinchu, Taiwan. NSRRC has a low-emittance, third-generation synchrotron radiation facility with a 1.5 GeV storage ring. The main character of the third-generation synchrotron radiation arrangement is its insertion devices (undulators, wigglers), which produce tunable VUV to soft X-ray radiation with much higher photon flux than bending magnets. The U9 beam line arrangement is operated by using an undulator of 4.5 m, providing $\sim 10^{16}$ photons/s VUV light for chemical dynamics research, and the photon energy could be tuned from 5 to 30 eV. The characteristics of this beamline are very similar to those of the chemical dynamics beamline at the Advanced Light Source (ALS) in Berkeley.[33]

VUV light as the ionization source has many advantages over the widely used electron impact ionization method. The tunable VUV ionization source could be used to reduce the magnitude of dissociative ionization of products and background species. In addition, the small heat load ($\sim$20 mW) allows the detection region to be easily cooled to liquid nitrogen temperature, making the inherent background much smaller in the detector. Photoionization also uses a much smaller ionization volume in comparison with the electron impact ionization, which provides higher resolution for product time-of-flight measurement.

The apparatus used in this study has been described in detail elsewhere.[34] It is also quite similar to the molecular beam apparatus on the chemical dynamics beam at ALS.[35] Several improvements have been made to increase the ionization transmission efficiency. In the photodissociation scheme of this apparatus, a pulsed molecular beam was crossed with a pulsed photolysis laser beam, and photofragments produced in the crossed region then entered the fixed detector and were detected with the synchrotron radiation. The sample of pure 1,3-butadiene was obtained from Fulgent Scientific Inc., and was used without further purification. A pulsed molecular beam of 1,3-butadiene was generated with a pulsed valve operating at 75 Hz. The stagnation pressure was maintained around 300 Torr. The molecular beam was introduced from the source region to the main chamber through two skimmers, and then intercepted by the 157 nm laser beam at a fixed angle of about 90°. The 157 laser beam was produced by a Lambda Physik LPF 200 F_2 laser with a NOVA tube laser cavity. The 1,3-butadiene beam, the pulsed laser beam, and the detection axis are all in the same plane. To avoid the multiphoton effect, the 157 nm laser power was attenuated by meshes to about 1−2 mJ/pulse in the experiment. The laser flux density was also reduced by focusing the laser beam by using a CaF_2 lens to a spot size of $\sim$3 mm $\times$ 7 mm in the section region. After flying about 10 cm from the crossed region, the neutral reaction products were then ionized by the synchrotron VUV photon ionizer. In this experiment, the synchrotron photon energy was tuned by adjusting the gap of the undulator device in the range from 28.5 to 36 mm, corresponding to 9.9−17.0 eV with a width of about 10% of the energy. The product ions guided from the ion optics were mass filtered by a quadrupole mass filter, and counted by a Daly ion detector. All TOF spectra were taken at 250 ns per channel during the experiment. The TOF spectra of the neutral photofragments measured in the laboratory frame were then converted to product translational energy distributions in the CM frame using the CMLAB3 and PHOTRAN simulation software developed by Harich.[36]

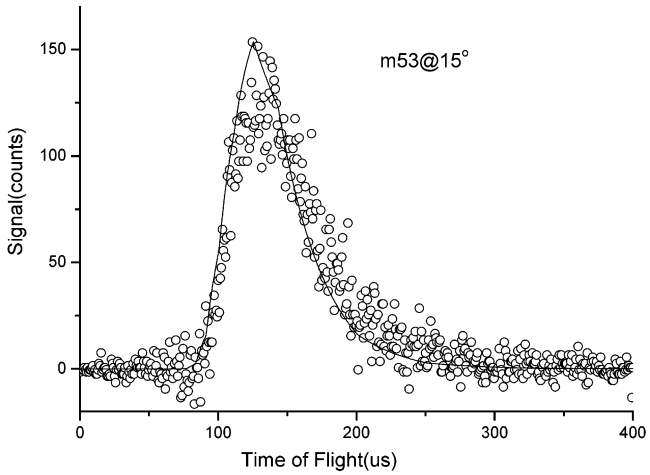

Figure 2. Time-of-flight spectra at $m/e = 53$ and $\theta = 15°$. The radical products were detected by direct ionization with 11 eV photons. The empty circles represent experimental data, while the solid curves are the fits to the spectra using the kinetic energy dissociation of the H atom elimination process shown in Figure 3.

III. Results and Discussion

TOF spectra of products produced in the photodissociation of 1,3-butadiene at 157 nm were measured using the experimental method described above. Signals of the photodissociation products from 1,3-butadiene photolysis at masses 1, 2, 15, 26, 27, 28, 39, 52, and 53 have been detected. Angular anisotropy of all observed photofragments (β parameter) has also been measured. Multiphoton effects were checked carefully. After careful measurements and detailed analyses of the TOF spectra, six dissociation channels were identified: $C_4H_5 + H$, $C_4H_4 + H + H$, $C_4H_4 + H_2$, $C_2H_4 + C_2H_2$, $C_2H_3 + C_2H_3$, and $C_3H_3 + CH_3$. Product translational energy distributions for all the channels have been determined. Angular anisotropy of all observed photofragments (β parameter) measured was zero. All the results are consistent with the picture that the dissociation of this molecule likely occurs on the ground state via internal conversion from the excited state.

H Formation Process: $C_4H_5 + H$ and $C_4H_4 + H + H$. A H atom detachment process from the 1,3-butadiene at 157 nm has been observed. Both the light fragment (H atom, mass 1) and its heavy partner (C_4H_5, mass 53) have been detected. Figure 2 shows the TOF spectra of the C_4H_5 product at the laboratory angle of 15°. It is clear that the product at mass 53 is from the binary dissociation channel of $C_4H_5 + H$ since there is no contribution from other possible channels. Translational energy distribution has been determined for this binary dissociation channel and is shown in Figure 3. Figure 4 shows the time-of flight spectrum of the H atom product at a laboratory angle of 30°. Using the translational energy distribution obtained from simulating the mass 53 TOF spectra, we have tried to simulate the TOF spectra for the H atom product. The binary H atom dissociation process only matches the fastest edge in the TOF for the H atom, indicating there are other sources of H atom products in addition to the binary H atom dissociation process.

Clearly, the triple dissociation channel, $C_4H_4 + H + H$, is another possible source of H atom product. The parent ion of

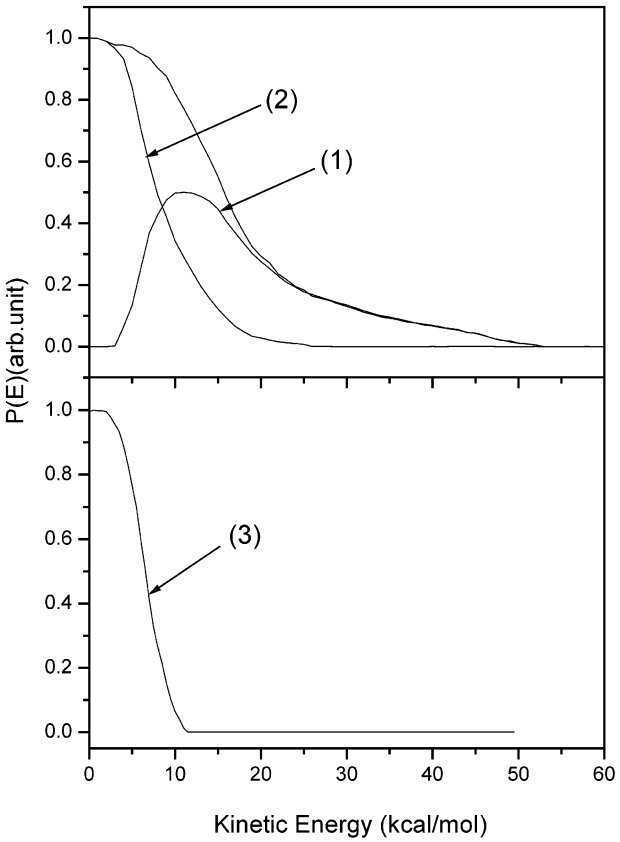

Figure 3. Primary and secondary translational energy distributions used in simulating the binary H atom channel, $C_4H_5 + H$, and the triple dissociation channel, $C_4H_4 + H + H$: (1) $P(E)$ for the binary H atom elimination process, (2) $P(E)$ for the primary H atom dissociation for the triple dissociation channel, (3) $P(E)$ for the secondary H atom dissociation for the triple dissociation channel.

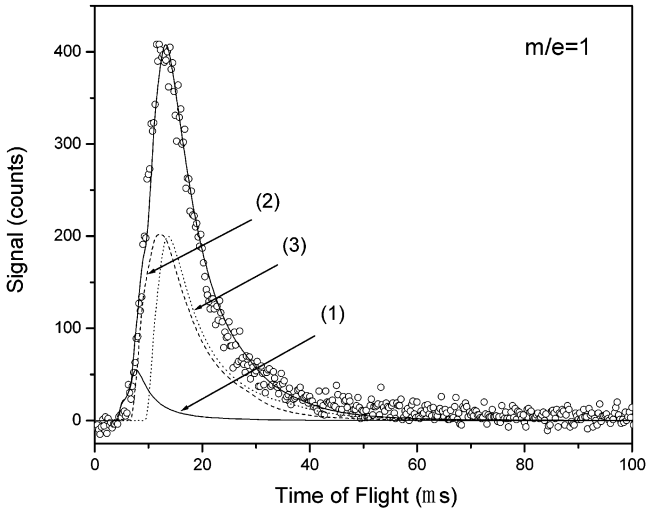

Figure 4. Time-of-flight spectrum at $m/e = 1$ and $\theta = 30°$. The radical products were detected by direct ionization with 17 eV photons. The open circles are the experimental data points, while the solid lines are simulated results. Key: (1) simple H atom elimination, momentum matched with the feature observed at mass 53, (2) H atom products from the primary dissociation process, $(C_4H_5)^* + H$, (3) H atom products from the secondary dissociation process of the hot $(C_4H_5)^*$ radical process, $(C_4H_5)^* \rightarrow C_4H_4 + H$.

the heavy fragment of this triple dissociation channel (C_4H_4) would appear at mass 52. Signals at this mass have also been observed. Figure 5 shows the TOF spectra of dissociation products appearing at mass 52 and $\theta = 15°$ and 30°. The TOF

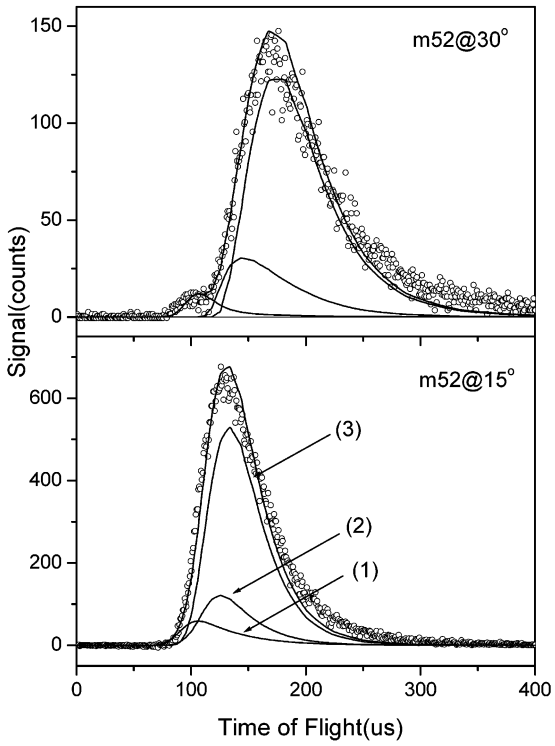

Figure 5. Time-of-flight spectrum at $m/e = 52$ and $\theta = 15°$ and 30° from the photodissociation of 1,3-butadiene. The radical products were detected by direct ionization with 11 eV photons. The open circles are the experimental data points, while the solid lines are the simulated contributions from three channels: (1) C_4H_4 product from H_2 elimination, (2) cracking of the C_4H_5 radical, (3) C_4H_4 product from the $C_4H_4 + H + H$ triple product channel.

spectra can be fitted satisfactorily using three contributions. The first two contributions are the H_2 elimination channel, which will be discussed in the next section, and the contribution of dissociative ionization from the radical product C_4H_5. The translational energy distributions for these two contributions are already known. However, it is not possible to simulate the TOF spectra at mass 52 using just these two contributions. The extra H atoms are likely due to the triple dissociation channel $C_4H_4 + 2H$. We have simulated this contribution assuming that the triple dissociation occurs stepwise by using a primary $P(E)$ to describe the $(C_4H_5)^* + H$ process and a secondary $P(E)$ to describe the secondary dissociation process of the hot $(C_4H_5)^*$ radical: $(C_4H_5)^* \rightarrow C_4H_4 + H$. The primary and secondary $P(E)$ functions obtained from simulating this third part are also shown in Figure 3. One can see that the primary $P(E)$ for the triple products is connected smoothly to the $P(E)$ obtained for the binary H atom channel obtained from the mass 53 product. This implies that the picture of the stepwise triple dissociation is reasonable. In this picture, a H atom is first eliminated from 1,3-butadiene, and the cold C_4H_5 radicals survive to fly to the detector while the hot C_4H_5 radicals go though a secondary dissociation to lose another H atom. The contribution of the primary and secondary H atom products can also be seen in the H atom TOF spectrum (Figure 4). Clearly, by including this triple dissociation, the TOF spectra at both mass 1 and mass 52 can be satisfactorily simulated, indicating that the existence of this triple dissociation is also reasonable.

H atom elimination from either central C−H bond gives buta-1,2-dien-4-yl (CH_2CHCCH_2), while H atom loss from either terminal CH_2 group will produce another isomer of the C_4H_5 radical buta-1,3-dien-4-yl ($CH_2CHCHCH$). It seems that H atom elimination from both sites may occur since these two channels

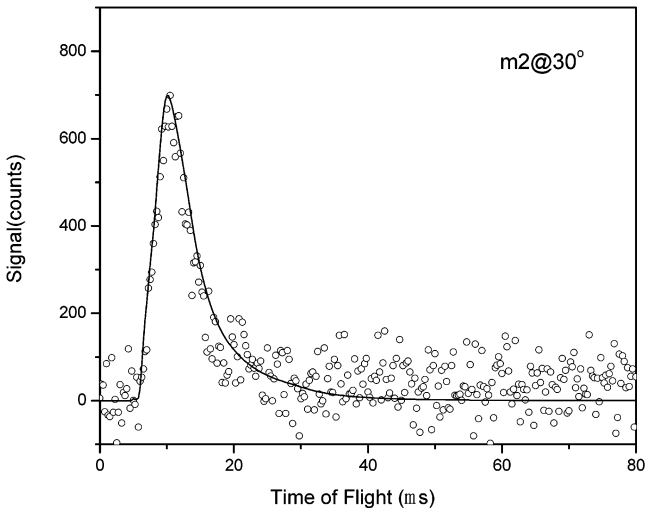

Figure 6. Time-of-flight spectrum at $m/e = 2$ and $\theta = 30°$. The dissociation products were detected by direct ionization with 17 eV photons. The open circles are the experimental data points, while the solid line is the simulated TOF spectrum from H_2 elimination.

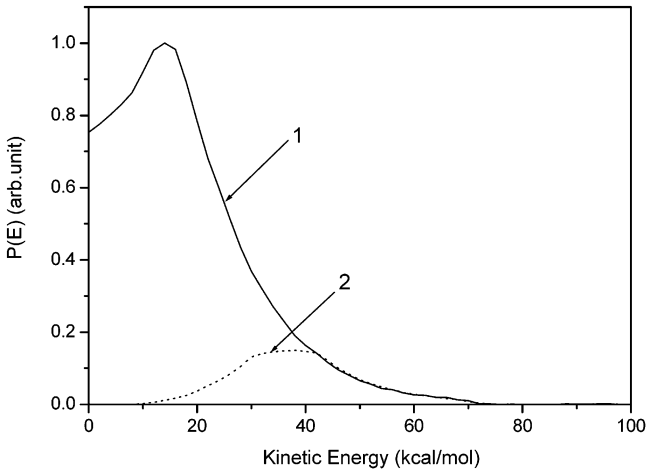

Figure 7. Translational energy distributions of the H_2 elimination channel from 1,3-butadiene photodissociation at 157 nm. Curve 1 is derived from the light product (mass 2), while curve 2 is obtained from fitting the fast peak in the TOF spectrum of the heavy product at mass 52.

are energetically very close. The work of Robinson et al. suggests that the buta-1,2-dien-4-yl channel, that is, the H atom channel from the two terminal CH_2 groups, is more favorable.[25] Buta-1,2-dien-4-yl could also lose another H atom from the CH_2 group to produce the vinylacetylene ($C_2HCHCCH$) product, with a barrier of 46.6 kcal/mol. The overall available energy for the buta-1,2-dien-4-yl product after primary photodissociation of the parent 1,3-butadiene molecule at 157 nm is 72.0 kcal/mol, and the maximal translational energy deposited in the radical to overcome the barrier for the secondary decomposition to occur is 48 kcal/mol. Therefore, secondary dissociation of the C_4H_5 product to form vinylacetylene + H is energetically accessible. This is also a very likely pathway for the triple dissociation process.

H_2 Formation Channel. A H_2 elimination process has also been observed from the photolysis of 1,3-butadiene at 157 nm. Time-of-flight spectra of the reaction products from this channel were measured. Figure 6 shows the TOF spectrum at $m/e = 2$. Translational energy distribution for the H_2 elimination process is determined by fitting the TOF spectrum using the CMLAB3 program. Figure 7 shows the translational energy distribution for the H_2 elimination. Signals at heavy mass product (mass 52) for this channel were also measured and are shown in Figure 5. The fast small peak shown in Figure 5 should come from the H_2 elimination channel. The translational energy distribution derived from the heavy fragment at mass 52, shown also in Figure 7, is however different from that derived from the H_2 TOF spectrum. It appears that the translational energy distribution derived from the heavy fragment at mass 52 only matches the fastest portion of the translational energy distribution derived from the H_2 product, implying that the slower heavy product at mass 52, or the more internally excited heavy product, is missing. There are two possible explanations. One possibility is that these internally hot heavy products produced from the binary elimination go through a secondary dissociation process. Another possibility is that the slower H_2 products are produced from some triple dissociation channels, such as $C_4H_3 + H + H_2$, while the faster products are produced from the binary H_2 elimination process. Energetically, these channels are accessible. Therefore, we could not exclude this possibility.

There are a few ways to eliminate a hydrogen molecule from 1,3-butadiene. One possible pathway is to eliminate molecular hydrogen via a four-center transition state, producing butatriene ($H_2C{=}C{=}C{=}CH_2$), in which the two hydrogen atoms are eliminated from two different carbons. Another possible pathway is the three-center elimination from the terminal carbons of 1,3-butadiene. This pathway produces vinylvinylidene ($:C{=}CH{-}CH{=}CH_2$), which could rearrange to the more stable vinylacetylene ($H{-}C{\equiv}C{-}CH{=}CH_2$) by a 1,2-H shift over a low barrier of about 4 kcal/mol. Energetically, the latter channel is more favorable. From the studies of molecular hydrogen elimination from ethylene, three-center eliminations are usually more favorable than four-center elimination.[25,37]

$C_3H_3 + CH_3$ Channel. Methyl elimination has also been detected from the photolysis of 1,3-butadiene at 157 nm. TOF spectra at mass 39 and mass 15 have been observed at laboratory angles of 15° and 30°, shown in Figure 8. The TOF spectra at mass 39 and mass 15 can be simulated using a single translational energy distribution for a binary dissociation channel, indicating that these signals are indeed due to the $C_3H_3 + CH_3$ channel from the dissociation of 1,3-butadiene. Figure 9a shows the translational energy distribution for the methyl elimination. We have obtained TOF spectra at mass 40, mass 38, mass 16, and mass 14. The signal at mass 40 is determined to be about 4% of that at mass 39 with the same shape, which is attributed to the ^{13}C isotopomer of the mass 39 product. Mass 14 can also be simulated using the translational energy distribution shown in Figure 9a; therefore, it is believed to be from the dissociative ionization of the methyl radical. From these analyses, the dissociation channel $CH_2 + C_3H_4$ is not observed here. This conclusion agrees with the theoretical study by Lee et al.[37] Similarly, the signal at mass 16 is determined to be about 1.5% of the signal at mass 15 with the same shape. Therefore, it is very likely that the mass 16 signals are all due to the ^{13}C isotopomer of the methyl radical. The mass 38 signal could be satisfactorily simulated using the translational energy distribution shown in Figure 9a, indicating that it is from the dissociative ionization of the mass 39 product. Therefore, there is no strong evidence here that the $CH_4 + H_2CCC$ channel is present. The $C_3H_3 + CH_3$ channel is clearly not produced from a direct bond cleavage of 1,3-butadiene. Rather, the 1,3-butadiene goes through an isomerization process first to 1,2-butadiene before it breaks into the $C_3H_3 + CH_3$ channel. According to the calculated isomerization rate and the dissociation rates,[37] the 1,3-butadiene → 1,2-butadiene isomerization is a faster process than other fragmentation pathways. This result strongly supports

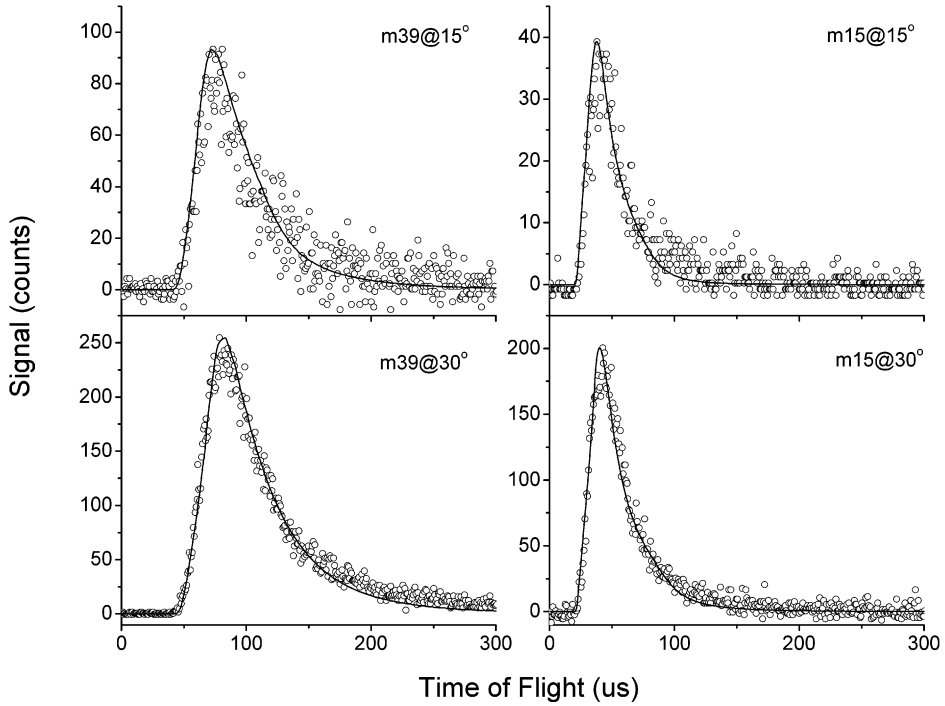

Figure 8. Time-of-flight spectra at $m/e = 39$, $m/e = 15$, and $\theta = 15°$ and 30° from the photodissociation of 1,3-butadiene at 157 nm. The radical products were detected by direct ionization with 11 eV photons. The open circles are the experimental data points, while the solid line is the simulation result using the kinetic energy distribution shown in Figure 10.

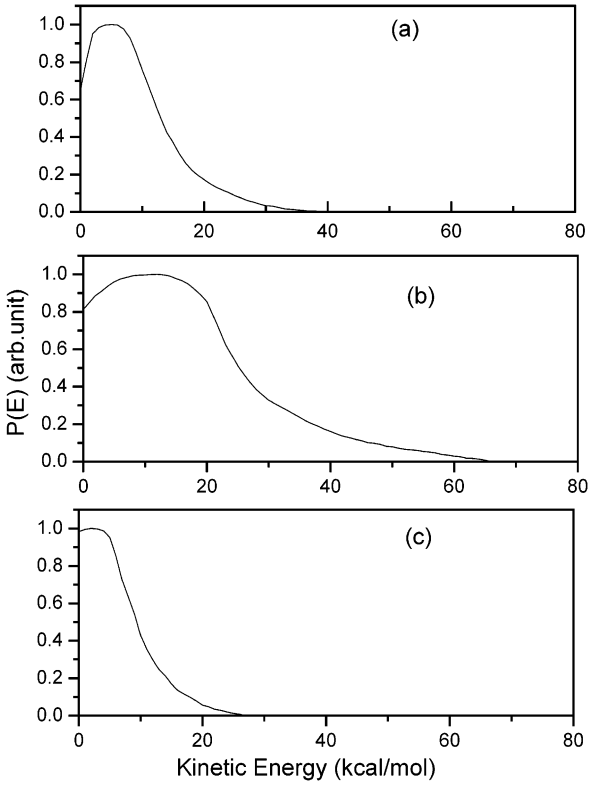

Figure 9. (a) Translational energy distribution of the methyl elimination channel from 1,3-butadiene photodissociation at 157 nm. (b) Translational energy distributions obtained by simulating the TOF spectra at masses 28 and 26. (c) Translational energy distribution for the C_2H_3 formation process.

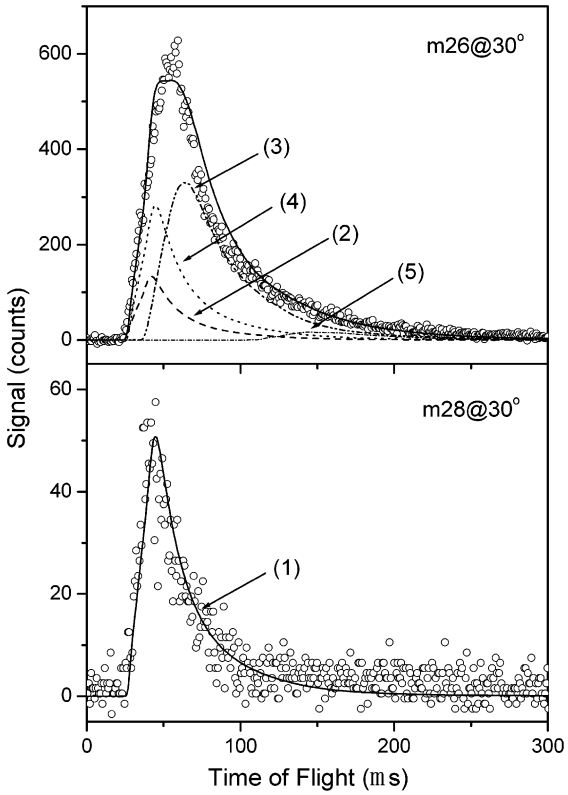

Figure 10. Time-of-flight spectrum at mass 28 and mass 26 from 1,3-butadiene photodissociation at 157 nm, detected at the 30° laboratory angle. The dissociation products were detected by direct ionization with 11.9 eV photons. The open circles are the experimental data points, while the solid lines are the simulated results with contributions from different sources: (1) C_2H_4 product from the C_2H_2 elimination, (2) C_2H_2 photoproduct, (3) cracking of the C_2H_3 radical to this mass, (4) cracking of C_2H_4 to this mass, (5) cracking of the C_4H_5 radical to this mass.

the physical picture for this channel in which isomerization occurs prior to the dissociation process.

C_2H_4 + C_2H_2 Channel. TOF spectra at masses 28 and 26 have also been observed in this work, shown in Figure 10. The TOF spectrum at mass 28 is simulated using the translational energy distribution shown in Figure 9b. It is not possible to fit the TOF spectrum at mass 26 by using only the translational

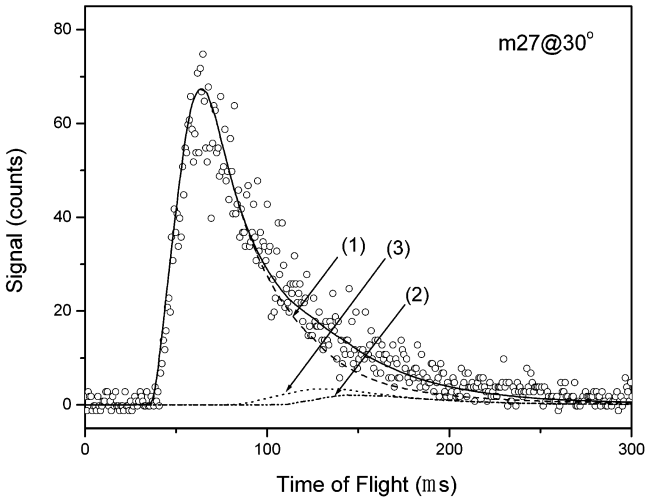

Figure 11. Time-of-flight spectrum at $m/e = 27$ and $\theta = 30°$ from 1,3-butadiene photodissociation. The dissociation products were detected by direct ionization with 9.45 eV photons. The open circles are the experimental data points, while the solid lines are the simulated contributions from three sources: (1) the fast peak in front corresponds to the C_2H_3 photoproduct, (2) cracking of the C_4H_5 radical to this mass, (3) cracking of C_4H_4 to this mass.

energy distribution shown in Figure 9a. The contribution of this channel, however, is clearly present, implying that the $C_2H_4 + C_2H_2$ channel is very likely present. By adding the contributions of dissociative ionization from masses 28, 27, and 53, a good fit for the TOF spectrum at mass 26 can be obtained. The formation of the $C_2H_4 + C_2H_2$ channel requires some rearrangement before dissociation; two possible microchannels are possible.[37] One pathway is via a 1,3-hydrogen migration from the terminal CH_2 group before the C−C bond breaking. The other pathway involves the isomerization of *trans*-1,3-butadiene to *cis*-1,3-butadiene and then cyclobutene before decomposition to $C_2H_4 + C_2H_2$. It seems that the former process via hydrogen migration should be more likely to occur because it is a more direct process.

$C_2H_3 + C_2H_3$ Channel. Figure 11 shows the TOF spectrum detected at mass 27. Since the fast peak is different from all other signals and could not be attributed to any other known channels, we have assigned the fast TOF signals to the $C_2H_3 + C_2H_3$ channel, a direct C−C bond breaking channel from 1,3-butadiene. The kinetic energy distribution for this channel can be obtained by fitting the TOF spectra at mass 27, and is shown in Figure 9c. In addition to the fast peak in the $m/e = 27$ TOF signals, there is also a slower peak which can be attributed to the dissociative ionization of the C_4H_5 and C_4H_4 radicals and simulated using the $P(E)$ functions shown in Figures 3 and 7. The formation of $C_2H_3 + C_2H_3$ is likely a simple C−C breaking process without going through isomerization for the 1,3-butadiene molecule.

Branching Ratios of Detected Dissociation Channels. In the present work, we have measured all the TOF signals that can be detected. The TOF signals for all primary products and cracking masses from the photodissociation of 1,3-butadiene have been analyzed, and normalized carefully. The laser power for each TOF spectrum was also well controlled. By accumulating the contributions of different fragment ions to each channel, the relative branching ratios of each dissociation pathway can be determined. Since the ionization cross-section of each dissociation fragment is unknown, the ionization photon energy was set quite high (about 17 eV) to mimic the ionization of electron impact ionization, in which the ionization efficiency for each observed fragment is more uniform than the threshold ionization condition. In estimating the branching ratios, we have assumed that the detection efficiency for each observed fragment is the same in such experimental conditions. The branching ratios thus obtained are listed in Table 1. Obviously, the $C_3H_3 + CH_3$ dissociation channel in this molecule is the most important process, with very significant contributions from the simple C−C bond fission process, $C_2H_3 + C_2H_3$, and the $C_2H_4 + C_2H_2$ channel, while atomic and molecular hydrogen related channels are unimportant. This result indicates that isomerization is very important in the photodissociation of 1,3-butadiene at 157 nm, in which the majority of the products are produced through isomerization. In comparison with the 1,2-butadiene results,[38] isomerization processes are certainly more important in 1,3-butadiene. It is certainly interesting to point out that the $C_3H_3 + CH_3$ channel is significantly less important in 1,3-butadiene than in 1,2-butadiene while the $C_2H_3 + C_2H_3$ channel and the $C_2H_4 + C_2H_2$ channel are significantly more important in this molecule. These observations are quite reasonable since the $C_3H_3 + CH_3$ channel is a direct single C−C bond dissociation in the 1,2-butadiene while this same channel occurs via an isomerization process prior to dissociation in the 1,3-butadiene molecule. The $C_2H_3 + C_2H_3$ channel is a direct C−C bond fission process in 1,3-butadiene, while this channel proceeds via 1,2-butadiene to 1,3-butadiene isomerization in 1,2-butadiene photolysis. Therefore, the $C_2H_3 + C_2H_3$ channel is more significant in 1,3-butadiene than 1,2-butadiene. The interesting observation that 1,3-butadiene photodissociation occurs mainly via an isomerization route while 1,2-butadiene photodissociation is mainly through direct bond dissociation is likely caused by the difference of the single C−C bond in the two molecules. The C−C bond in 1,2-butadiene is weaker than the C−C bond in 1,3-butadiene; therefore, direct C−C dissociation is easier in 1,2-butadiene than in 1,3-butadiene. Obviously, the direct C−C dissociation wins out in 1,2-butadiene in competition with isomerization, while isomerization is faster in 1,3-butadiene in competing with direct bond dissociation processes.

TABLE 1: Branching Ratios of All Observed Dissociation Channels

dissociation channel	branching ratio (%)	dissociation channel	branching ratio (%)
$C_4H_5 + H$	0.7	$C_3H_3 + CH_3$	46
$C_4H_4 + H_2$	2.2	$C_2H_4 + C_2H_2$	14
$C_4H_4 + H + H$	8.5	$C_2H_3 + C_2H_3$	28.6

In 193 nm photodissociation of 1,3-butadiene, five dissociation channels have been observed. The branching ratio of the five channels, $C_4H_5 + H$:$C_4H_4 + H_2$:$C_3H_3 + CH_3$:$C_2H_4 + C_2H_2$:$C_2H_3 + C_2H_3$, is determined to be 20:2:50:20:8 by Robinson[25] et al., and the corresponding branching ratio calculated by Mebel et al. is 24.0:6.1:49.6:15.2:4.6.[37] In comparison with the photodissociation at 157 nm in this work, the triple dissociation channel, $C_4H_4 + H + H$, is not observed at 193 nm. The branching ratios for the $C_4H_5 + H$ and $C_2H_3 + C_2H_3$ channels are significantly different from the results of dissociation at 193 nm, indicating the competitive nature of the different channels at different energies. For the H atom channel, the overall H atom relative branching at 157 nm should be the sum of the relative branching of the binary H atom and that of the triple channel, which is 9.2%. This is about half of that in the photodissociation at 193 nm. For the $C_2H_3 + C_2H_3$ channel, the relative branching becomes significantly more important at 157 nm in comparison with that at 193 nm. This is likely due to the competitive nature of the different dissociation channels

at different energies. The detailed mechanism for these changes needs further theoretical investigation of the energetics as well as the characteristics of potential energy surfaces. The relative importance of other channels seems to be more or less the same for the photodissociation at the two wavelengths. From the translational energy distributions at 157 nm, it seems that most of the excess 1.47 eV energy in comparison with that of 193 nm excitation appears in the internal degrees of freedom in the molecular products.

IV. Conclusions

We have investigated the photodissociation of 1,3-butadiene at 157 nm by using the technique of photofragment translational spectroscopy. TOF spectra for photofragments at $m/e = 1$, 2, 15, 26, 27, 28, 39, 52, and 53 have been measured. Analysis of these experimental results reveals six different dissociation channels: (1) $C_4H_5 + H$, (2) $C_4H_4 + H_2$, (3) $C_3H_3 + CH_3$, (4) $C_2H_3 + C_2H_3$, (5) $C_2H_4 + C_2H_2$, (6) $C_4H_4 + H + H$. Translational energy distributions for all observed dissociation channels were determined. Branching ratios for all observed channels were also estimated. It appears that C−C bond breaking channels are the dominant processes in the photodissociation of 1,3-butadiene at 157 nm, in which the majority of these processes occur via isomerization prior to dissociation. This picture is significantly different from that of the 1,2-butadiene photodissociation at 157 nm.

Acknowledgment. This work was supported by the NSFC (Grant No. 20273071), the Academia Sinica, the National Synchrotron Radiation Research Center in Taiwan, and the Chinese Academy of Sciences.

References and Notes

(1) McDiarmid, R. *J. Chem. Phys.* **1976**, *64*, 514.
(2) McDiarmid, R.; Sheybani, A. H. *J. Chem. Phys.* **1988**, *89*, 1255.
(3) Mallard, W. G.; Miller, J. H.; Smyth, K. C. *J. Chem. Phys.* **1983**, *79*, 5900.
(4) Taylor, P. H.; Mallard, W. G.; Smyth, K. C. *J. Chem. Phys.* **1986**, *84*, 1053.
(5) Nascimento, M. A. C.; Goddard, W. A., III *Chem. Phys.* **1979**, *36*, 147.
(6) Hollauer, E.; Nascimento, M. A. C. *J. Chem. Phys.* **1980**, *88*, 7245.
(7) Serrano-Andrés, L.; Merchán, M.; Nebot-Gil, I. *J. Chem. Phys.* **1993**, *98*, 3151.
(8) Watts, J. D.; Gwaltney, S. R.; Bartlett, R. J. *J. Chem. Phys.* **1996**, *105*, 6979.
(9) Liu, J.; Anderson, S. L. *J. Chem. Phys.* **2001**, *114*, 6618.
(10) Graham, R. L.; Freed, K. F. *J. Chem. Phys.* **1992**, *96*, 1304.
(11) Wiberg, K. B.; Hadad, C. M.; Ellison, G. B.; Foresman, J. B. *J. Phys. Chem.* **1993**, *97*, 13586.
(12) Collin, J. F.; Lossing, P. *Can. J. Chem.* **1957**, *35*, 778.
(13) Srinivasan, R. *Adv. Photochem.* **1966**, *4*, 113.
(14) Haller, I.; Srinivasan, R. *J. Chem. Phys.* **1964**, *40*, 1992.
(15) Haller, I.; Srinivasan, R. *J. Am. Chem. Soc.* **1966**, *88*, 3694.
(16) Doepker, R. D. *J. Phys. Chem.* **1968**, *72*, 4037.
(17) Collin, G. J.; Deslauriers, H. G.; Maré, R. D.; Poirer, R. A. *J. Phys. Chem.* **1990**, *94*, 134.
(18) Skinner, G. B.; Sokoloski, E. M. *J. Phys. Chem.* **1960**, *64*, 1028.
(19) Kiefer, J. H.; Wei, H. C.; Kern, R. D.; Wu, C. H. *Int. J. Chem. Kinet.* **1985**, *17*, 225.
(20) Kiefer, J. H.; Mitchell, K. I.; Wei, H. C. *Int. J. Chem. Kinet.* **1988**, *20*, 787.
(21) Rao, V. S.; Takeda, K.; Skinner, G. B. *Int. J. Chem. Kinet.* **1988**, *20*, 153.
(22) Kiefer, J. H.; Kumaran, S. S.; Mudipalli, P. S. *Chem. Phys. Lett.* **1994**, *224*, 51.
(23) Hidaka, Y.; Higashihara, T.; Ninomiya, N.; Masaoka, H.; Nakamura, T.; Kawano, H. *Int. J. Chem. Kinet.* **1996**, *28*, 137.
(24) Venkataraman, B. K.; Valentini, J. J. *Chem. Phys. Lett.* **1992**, *194*, 191.
(25) Robinson, J. C.; Harris, S. A.; Sun, W.; Sveum, N. E.; Neumark, D. M. *J. Am. Chem. Soc.* **2002**, *124*, 10211.
(26) Nguyen, T. T.; King, K. D. *Int. J. Chem. Kinet.* **1982**, *14*, 613.
(27) Lias, S. G.; Bartmas, J. E.; Liebman, J. F.; Holmes, J. L.; Levin, R. D.; Mallard, W. G. *J. Phys. Chem. Ref. Data* **1988**, *17*, 872.
(28) Ervin, K. M.; Gronert, S.; Barlow, S. E.; Gilles, M. K.; Harrison, A. G.; Bierbaum, V. M.; Depuy, C. H.; Lineberger, W. C.; Ellison, G. B. *J. Am. Chem. Soc.* **1990**, *112*, 5750.
(29) Parker, C. L.; Cooksy, A. L. *J. Phys. Chem. A* **1999**, *103*, 2160.
(30) Robinson, M. S.; Polak, M. L.; Bierbaum, V. M.; Depuy, C. H.; Lineberger, W. C. *J. Am. Chem. Soc.* **1995**, *117*, 6766.
(31) Gilbert, T.; Pfab, R.; Fischer, I.; Chen, P. *J. Chem. Phys.* **2000**, *112*, 2575.
(32) *NIST Chemistry Webbook*; National Institute of Standards and Technology: Gaithersburg, MD, 2000; http://webbook.nist.gov/chemistry/.
(33) Heimann, P. A.; Koike, M.; Hsu, C. W. *Rev. Sci. Instrum.* **1997**, *68*, 1945.
(34) Lin, J.; Huang, D. W.; Harich, S.; Lee, Y. T.; Yang, X. *Rev. Sci. Instrum.* **1998**, *69*, 1642.
(35) Yang, X.; Blank, D. A.; Lin, J.; Suits, A. G.; Lee, Y. T.; Wodtke, A. M. *Rev. Sci. Instrum.* **1997**, *68*, 3317.
(36) Harich, Steven A. Ph.D. Thesis, Department of Chemistry, University of California at Santa Barbara, 1999.
(37) Lee, H. Y.; Kislov, V. V.; Lin, S. H.; Mebel, A. M.; Neumark, D. M. *Chem.−Eur. J.* **2003**, *9*, 726.
(38) Mu, X. L.; Lu, I.-C.; Lee, S.-H.; Wang, X. Y.; Yang, X. *J. Chem. Phys.* **2004**, *121*, 4684.